






LGALS3BP is a potential target of antibody-drug conjugates in oral squamous cell carcinoma

Ilaria Cela^{1,2}  | Vito Carlo Alberto Caponio³  | Emily Capone^{1,2} | Morena Pinti⁴ | Marco Mascitti⁵ | Lucrezia Togni⁵ | Lorenzo Lo Muzio³  | Corrado Rubini⁶ | Vincenzo De Laurenzi^{1,2} | Rossano Lattanzio^{1,2}  | Vittoria Perrotti⁴ | Gianluca Sala^{1,2} 

¹Department of Innovative Technologies in Medicine & Dentistry, "G. d'Annunzio" University of Chieti-Pescara, Chieti, Italy

²Center for Advanced Studies and Technology (CAST), "G. d'Annunzio" University of Chieti-Pescara, Chieti, Italy

³Department of Clinical and Experimental Medicine, University of Foggia, Foggia, Italy

⁴Department of Medical, Oral and Biotechnological Sciences, "G. d'Annunzio" University of Chieti-Pescara, Chieti, Italy

⁵Department of Clinical Specialistic and Dental Sciences, Marche Polytechnic University, Ancona, Italy

⁶Department of Biomedical Sciences and Public Health, Marche Polytechnic University, Ancona, Italy

Correspondence

Gianluca Sala, Laboratory of Clinical Biochemistry and Molecular Biology, Center for Advanced Studies and Technology (CAST), "G. d'Annunzio" University of Chieti-Pescara, Via L. Polacchi 11, Chieti 66110, Italy.
Email: g.sala@unich.it

Vittoria Perrotti, Department of Medical, Oral and Biotechnological Sciences, "G. d'Annunzio" University of Chieti-Pescara, Via dei Vestini 31, Chieti 66100, Italy.
Email: v.perrotti@unich.it

Funding information

Fondazione-AIRC, Grant/Award Number: IG 2018 id 20043 and IG 2021 id 25696

Abstract

Objective: The aim of the present study was to evaluate the expression of intracellular and vesicular LGALS3BP in oral squamous cell carcinoma (OSCC) patients and available cell lines to explore its potential as a target for antibody-drug conjugate (ADC) therapy.

Methods: Free and vesicular LGALS3BP expression levels were evaluated in cancer tissues from a cohort of OSCC patients as well as in a panel of OSCC cell lines through immunohistochemistry, qRT-PCR, Western Blot analysis, and ELISA.

Results: LGALS3BP resulted in being highly expressed in the cytoplasm of tumour cells in OSCC patient tissues. A strong correlation was found between high LGALS3BP expression levels and aggressive histological features of OSCC. Biochemistry analysis performed on OSCC cell lines showed that LGALS3BP is expressed in all the tested cell lines and highly enriched in cancer-derived extracellular vesicles. Moreover, LGALS3BP high-expressing HOC621 and CAL27 OSCC cell lines showed high sensitivity to the ADC-payload DM4, with an IC_{50} around 0.3 nM.

Conclusions: The present study highlights that LGALS3BP is highly expressed in OSCC suggesting a role as a potential diagnostic biomarker and therapeutic target for ADC-based therapy.

KEYWORDS

antibody-drug conjugates, Galectin-3-binding protein, immunoconjugates, LGALS3BP protein, mouth neoplasms, oral squamous cell carcinoma, tumour biomarkers

Vittoria Perrotti and Gianluca Sala share senior authorship.

This is an open access article under the terms of the [Creative Commons Attribution-NonCommercial-NoDerivs](https://creativecommons.org/licenses/by-nc-nd/4.0/) License, which permits use and distribution in any medium, provided the original work is properly cited, the use is non-commercial and no modifications or adaptations are made.

© 2023 The Authors. *Oral Diseases* published by Wiley Periodicals LLC.

1 | INTRODUCTION

Oral squamous cell carcinoma (OSCC) is the most common malignant neoplasm affecting oral cavity, accounting for more than 90% of all oral cancers. Annually, over 300,000 cases are newly diagnosed, with a short-term survival rate of about 65% and a 5-year survival rate still hovering around 50% (Mascitti et al., 2020, 2022; Togni et al., 2022). Despite improvements in the knowledge of this disease and recent progress made in radiotherapy (RT), chemotherapy (CT) and conventional surgery, the overall survival (OS) has not essentially increased in the last decades mainly due to a poor response to standard anti-cancer treatments. Moreover, OSCC patients often experience notable complications related to treatment resistance and disease recurrence. Finally, the lack of valuable biomarkers that predict aggressiveness and recurrence risk together with scarceness of therapeutical targets make this scenario even more dismal (Zhang et al., 2019).

Hence, there is an urgent need to establish new therapies tailored to specific targets or pathways involved in OSCC tumorigenesis and ADC has assumed a primary role in the targeted therapy approach (Perrotti et al., 2021). In this context, the human lectin galactoside-binding soluble 3-binding protein (LGALS3BP) has emerged as an attractive target for a variety of cancers (Capone et al., 2021) due to its abundant expression on tumour tissue and its multifaced role as tumour-promoting factor. LGALS3BP (also known as Gal-3BP, 90K or Mac2-BP) is a secreted multifunctional glycoprotein expressed by several cancerous specimens, while undetectable or poorly present in normal tissues (Capone et al., 2020, 2021; Fornarini et al., 2000; Hee Lee et al., 2013; Ozaki et al., 2004; Park et al., 2007; Ulmer et al., 2006; Zhang et al., 2019). LGALS3BP is involved in immunity, angiogenesis, cellular adhesion and migration and tumour microenvironment (TME) crosstalk, influencing tumour growth and progression (Capone et al., 2021). Recently, LGALS3BP has been indicated as one of the most abundant glycoproteins on the surface of extracellular vesicles (EVs) derived from ovarian cancer, endometrial cancer, pancreatic ductal adenocarcinoma, glioblastoma and neuroblastoma (Capone et al., 2020; Castillo et al., 2018; Dufrusine et al., 2023; Escrevente et al., 2013; Nakata et al., 2017; Song et al., 2021) and implicated in cargo delivery of these vesicles (Zhu et al., 2023), proposing a functional specialization for vesicular LGALS3BP. Interestingly, LGALS3BP was previously shown to affect cell growth and motility of OSCC cells by likely acting as an oncogene (Endo et al., 2013; Weng et al., 2008; Zhang et al., 2019). In addition, overexpression of secreted LGALS3BP in OSCC cell lines was described (Fukamachi et al., 2018); more importantly, LGALS3BP from both serum and tissue of OSCC patients was significantly correlated with unfavourable prognosis (Weng et al., 2008), besides its role as a disease biomarker in saliva of OSCC patients (Singh et al., 2020; Yu et al., 2016).

Our group has recently developed a specific and potent maytansine derivative-based ADC targeting LGALS3BP—named 1959-sss/DM4—that has shown promising therapeutical efficacy in preclinical

models of melanoma, neuroblastoma and glioblastoma (Capone et al., 2020; Dufrusine et al., 2023; Giansanti et al., 2019). This compound was designed as a non-internalizing ADC able to target secreted LGALS3BP which accumulates in the tumour extracellular milieu. The DM4 maytansinoid derivative is a tubulin polymerization inhibitor characterized by lipophilic properties displaying a potent cell-killing activity in the picomolar range. Indeed, the reducing conditions of the tumour microenvironment (TME) may lead to the release of the cytotoxic payload (SH-DM4) which is site-specific conjugated through a disulfide bond to the C-terminal cysteine residue of each light chain of 1959sss antibody.

Interestingly, both naked and DM4-conjugated 1959 antibodies showed the ability to act as radioimmunoconjugates for ⁸⁹Zr-immunoPET, thus suggesting that both probes could play a role in the clinical imaging of LGALS3BP-expressing malignancies (Keinänen et al., 2023).

Given the urgency of developing novel therapeutic strategies for OSCC treatment and given the LGALS3BP potential as a druggable target, the purpose of the present study was to evaluate the expression of LGALS3BP in a cohort of OSCC to explore any possible correlation with clinical-pathological characteristics. Moreover, EVs-associated LGALS3BP expression was analysed in a panel of available OSCC cell lines to assess its potential as a druggable target for ADC-based therapy.

2 | MATERIALS AND METHODS

2.1 | Cell lines

OSCC cell lines HSC3, HSC4 and HSC2 were cultured in E-MEM (Eagle's Minimum Essential Medium, Gibco, Waltham, MA, USA); HOC621 and CAL27 cell lines were cultured in DMEM (Dulbecco's Minimum Essential Medium, Gibco, Waltham, MA, USA); SAS cell line was cultured in DMEM/F12 (Gibco, Waltham, MA, USA) and A253 cell line was cultured in McCoy's 5A (Gibco, Waltham, MA, USA). All the culture media were supplemented with 10% heat-inactivated foetal bovine serum (FBS, Gibco, Waltham, MA, USA), 100 units/mL penicillin and 100 µg/mL streptomycin (Sigma-Aldrich Corporation, St. Louis, MO, USA). HSC2, HSC3, HSC4, HOC621, CAL27 and SAS cell lines were a gift of Prof. Lorenzo Lo Muzio (University of Foggia, Italy); A253 cell line was purchased from American Type Culture Collection (ATCC #HTB-41, Rockville, MD, USA). HSC3, HSC4, HOC621, CAL27 and SAS cell lines derived from human tongue carcinoma, while HSC2 is from mouth floor carcinoma and A253 is from salivary glands carcinoma. Human gingival fibroblasts (hGF) were purchased from CLS (#300703; GmbH) and cultured in DMEM/F12 supplemented with heat-inactivated 5% FBS, 100 units/mL penicillin and 100 µg/mL streptomycin (Sigma-Aldrich Corporation, St. Louis, MO, USA). All cell lines were cultivated at most for 1 month and maintained at 37°C in a humidified air with 5% CO₂. All cell lines were tested for mycoplasma contamination through PCR.



2.2 | Patients

A cohort of randomly selected patients with OSCC was identified. Patients' charts were retrospectively screened for clinic-pathological information. Patients were originally treated at the Department of Maxillofacial Surgery, 'Ospedali Riuniti' General Hospital (Ancona, Italy) between 1990 and 2016. Surgical resection with curative intent was performed in all patients. Diagnostic slides were retrieved, and an assessment was performed to the updated staging system. All patients were staged according to the 8th AJCC Tumor Node Metastasis (TNM) Staging system. To be eligible for inclusion, the following criteria had to be met:

1. Primary OSCC, such as International Classification of Disease-10 (ICD) codes 00, 02, 03, 04, 05 and 06;
2. Over 18 years old at the time of diagnosis;
3. Absence of Human Papilloma Virus (HPV) infection.

Cases collected originally from relapsing, metastasizing or secondary primary tumours were excluded as well as those collected just after neoadjuvant treatment. The study was approved and reviewed by the Institutional Review Board of Regione Abruzzo (richk5st2 of 21.4.2023). All patients provided written consent for the use of their specimens for research purposes and the study was conducted in accordance with the 'Ethical Principles for Medical Research Involving Human Subjects' statement of the Helsinki Declaration. The clinical endpoint examined was overall OS. Follow-up was considered the time in months from the day in which the patient underwent surgical excision to the last check-follow-up alive status or death for any reason.

2.3 | Western blotting

A total of 5×10^5 OSCC cells and hGF were cultured in a complete medium for 48 h, then they were harvested. Pellet cells were lysed in RIPA buffer (50 mM Tris/HCl pH 7.6, 150 mM NaCl, 1% NP-40, 0.5% Na-Deoxycholate, 0.1% SDS, 1 mM EDTA pH 8) containing a protease inhibitor cocktail (Sigma-Aldrich, St. Louis, MI, USA), a phosphatase inhibitor cocktail (Roche, Thermo-Fisher, Waltham, MA, USA) and Na_3VO_4 (Sigma-Aldrich, St. Louis, MI, USA). Lysates were clarified by centrifugation at 13,000 rpm for 30 min at 4°C. Equal amounts of protein lysates (20 µg per sample) were subjected to 10% or 15% SDS-PAGE electrophoresis and then electrotransferred to nitrocellulose membranes for Western blot analysis. Membranes were blocked for 1 h at RT with 5% (g/v) non-fat dry milk in PBS with 0.1% (v/v) Tween20. Membranes were then incubated overnight at 4°C with the following primary antibodies: anti-human LGALS3BP (goat polyclonal; 1:1000, #AF2226, R&D Systems, Minneapolis, MN, USA), anti-human lectin, mannose-binding 1 (LMAN1) (rabbit monoclonal; 1:1000, EPR6979, ab125006, Abcam, Cambridge, UK), anti-human Multiple Coagulation Factor Deficiency 2 (MCFD2) (#294301) (mouse monoclonal; 1:500, MAB-2357,

R&D Systems, Minneapolis, MN, USA), anti-human β -actin (mouse monoclonal; 1:40000, A5441, Sigma-Aldrich, St. Louis, MI, USA). After three washes in PBS-0.1% (v/v) Tween20, the membranes were hybridized with horseradish peroxidase (HRP)-conjugated secondary antibodies (goat, rabbit, or mouse; Biorad, Hercules, CA, USA). Detection of signal bands was performed with Clarity Western ECL substrate (#1705061; Biorad, Hercules, CA, USA) or with a SuperSignal West Dura extended duration substrate kit (#34076; Thermo Fisher Scientific). Images of membranes were acquired with a UvitecFire reader (Cambridge, UK) and analysed with Alliance Uvitec software (Cambridge, UK).

2.4 | Quantitative reverse transcription-PCR (qRT-PCR)

A total of 5×10^5 OSCC cells and hGF were cultured in a complete medium for 48 h, then total RNA was isolated from collected cells by RNeasy kit (#74136, Qiagen, Hilden, Germany). One microgram of total RNA was reverse transcribed to cDNA by using a High-Capacity cDNA Reverse Transcription kit (#4368814; Applied Biosystems, Waltham, MA, USA), according to the manufacturer's instructions. Real-time qPCR was performed with a CFX96 Touch Real-Time PCR Detection system (Biorad, Hercules, CA, USA) using SsoAdvanced Universal SYBR Green supermix (#1725271; Biorad, Hercules, CA, USA), according to the manufacturer's instructions. The primers used at a final concentration of 350 nM were hLGALS3BP FOR 5'-GAACCCAAGGCGTGAACGAT-3', hLGALS3BP REV 5'-GTCCACA GGTGTACACACA-3', h- β -actin FOR 5'-CAGCTACCATGGATGATGATATC-3' and h- β -actin REV 5'-AAGCCGGCCTTGACAT-3'.

Each sample analysis was performed in triplicate. As a negative control, a no template control was performed. The following PCR program was used: 95°C for 30 s, 40 cycles of denaturation at 95°C for 15 s and annealing/extension at 57°C for 30 s. In order to verify the specificity of the amplification, a melting curve analysis was performed immediately after the amplification protocol. qRT-PCR results were calculated using the $\Delta\Delta\text{Ct}$ method, with β -actin used as a housekeeping reference gene.

2.5 | Enzyme-linked immunosorbent assay (ELISA)

A total of 5×10^5 OSCC cells and hGF were cultured in a complete medium for 48 h, then supernatants were collected. Sandwich ELISA for secreted LGALS3BP was performed as follows: Maxisorp 96-well plates were coated with murine anti-LGALS3BP antibody SP2 (Traini et al., 2014) [2 µg/mL] overnight at 4°C. After blocking with 1% (g/v) BSA in PBS for 1 h, 100 µL of supernatants were added and incubated for 1 h at RT. After three washes with PBS-0.05% (v/v) Tween20, humanized anti-LGALS3BP antibody 1959 [1 µg/mL] was incubated for 1 h at RT. For the detection, after three washes with PBS-0.05% (v/v) Tween20, anti-human IgG-HRP (#A01070, Sigma-Aldrich, St. Louis, MI, USA) was added

(1:5000) and incubated for 1 h at RT. After three washes, stabilized chromogen was added for at least 10 min in the dark, before stopping the reaction with the addition of 1 N H₂SO₄. The resulting color was finally read at 450 nm with an ELISA plate reader (Tecan, Männedorf, Switzerland).

2.6 | Extracellular vesicles purification and analysis

Once reached the 80% confluence, OSCC cell lines were cultivated for 48 h in a serum-free medium. Around 100 mL of cell culture supernatant were collected, and differential ultracentrifugation was performed for EVs isolation. Briefly, supernatants were centrifuged at 300g, 2000g and 10,000g for 10, 10 and 30 min, respectively, at 4°C to remove dead cells and cellular debris. Then, supernatants were ultracentrifuged at 100,000g for 70 min at 4°C in order to collect exosomes that were washed with PBS and re-collected by another centrifugation at 100,000g for 70 min at 4°C. Protein content of obtained exosomes was quantified by Bradford assay (Biorad, Hercules, California, USA) in 96-well plates that were read at 595 nm prior to analysis by Western blotting, besides whole-cell lysates previously lysed in RIPA lysis buffer as previously described. Briefly, whole-cell lysates and isolated EVs were prepared in a reducing or non-reducing sample buffer (without 2-mercaptoethanol, for CD9 and CD63 immunoblotting) and heated at 95°C for 10 min. Non-reduced blots were probed with primary antibodies anti-human CD9 (ALB 6) (mouse monoclonal; 1:200, sc-59140, SantaCruz Biotechnology, Dallas, TX, USA) and anti-human CD63 (RFAC4) (mouse monoclonal; 1:1000, #CBL553, Merck Millipore, Burlington, Massachusetts, USA). Reduced blots were probed with anti-human LGALS3BP antibody (goat polyclonal; 1:1000, #AF2226, R&D Systems, Minneapolis, MN, USA) and with anti-human β-actin (mouse monoclonal; 1:40000, Sigma-Aldrich, St. Louis, MI, USA). All primary antibodies were incubated overnight at 4°C; membranes were then probed with HRP-conjugated secondary antibodies (goat or mouse; Biorad, Hercules, CA, USA) for 1 h at RT. Blots were developed with a chemiluminescence system as previously described.

2.7 | Cytotoxicity assay

For cytotoxicity assay, CAL27 and HOC621 were cultivated into 24-well plates at a density of 9×10^3 /well and 8×10^3 /well, respectively, under standard growth conditions at 37°C in 5% CO₂. After 24 h, cells were treated for 72 h with increasing doses of SH-DM4 (Cod. HY-12454, MedChemExpress, New Jersey, USA) (ranging from 0.0032 nM to 50 nM). At the end of the treatment period, cells were incubated with 3-(4,5-dimethylthiazol-2-yl)-2,5-diphenyltetrazolium bromide (MTT) solution (medium serum-free with 0.5 mg/mL of MTT) for 2 h. After the removal of the MTT solution, dimethyl sulfoxide (DMSO) was added to each well and then the absorption value at 570 nm was measured using a multi-plate reader (Tecan). All

experiments were performed in triplicate and as three independent experiments. IC₅₀ (Inhibition of Cellular Proliferation by 50%) values were calculated by using GraphPad Prism 9.0 software (GraphPad Software, Inc., San Diego, CA, USA).

TABLE 1 Characteristics of patients with oral squamous cell carcinoma (OSCC) (*n* = 98).

Variable	Value (%)
Age at diagnosis (year)	
Mean ± SD	66.0 ± 12.9
Median (range)	68.0 (26–88)
Gender	
Male	79 (80.6)
Female	19 (19.4)
Tumour location	
Tongue	63 (64.3)
Gingiva	2 (2.0)
Mouth's floor	8 (8.2)
Palate	1 (1.0)
Cheek	24 (24.5)
Tumour stage	
I	27 (27.6)
II	22 (22.4)
III	18 (18.4)
IV	29 (29.6)
Unknown	2 (2.0)
Tumour grade	
1	24 (24.5)
2	47 (48.0)
3	25 (25.5)
Unknown	2 (2.0)
LVI	
Absent	88 (89.8)
Present	9 (9.2)
Unknown	1 (1.0)
DOI (mm)	
<5	25 (26.5)
5–10	20 (20.4)
>10	5 (5.1)
Unknown	48 (49.0)
WPOI	
Grade 1	26 (26.5)
Grade 2	11 (11.2)
Grade 3	39 (39.8)
Grade 4	20 (20.4)
Grade 5	1 (1.0)
Unknown	1 (1.0)

Abbreviations: DOI, depth of invasion; LVI, lymphovascular invasion; WPOI, worst pattern of invasion.



2.8 | Immunohistochemistry (IHC)

OSCC tissue sections were stained with a goat polyclonal antibody raised against human LGALS3BP (goat polyclonal; 1:400 dilution; 60' incubation; #AF2226, R&D Systems, Minneapolis, MN, USA). Antigen retrieval was performed by microwave treatment at 750W (10min) in citrate buffer (pH6.0). The ABC kit was used for signal amplification. DAB (3,3'-Diaminobenzidine) was used as the chromogen.

2.9 | Statistical analysis

The chi-square test was used to investigate the relationships between LGALS3BP expression and the clinical-pathological parameters of patients. Based on the median value of expression of 83% at IHC, patients were categorized in high and low expression for

LGALS3BP. Kaplan–Meier analysis was performed to estimate OS by log-rank test and represented by survival curves. Variables impacting OS in univariate analysis (p -value <0.150) were considered to build the multivariate model on Cox regression analysis.

3 | RESULTS

3.1 | Immunohistochemical evaluation of LGALS3BP expression in oral squamous cell carcinoma

LGALS3BP protein expression in OSCC was evaluated by IHC in 98 cases. Patients and tumour characteristics are summarized in Table 1. LGALS3BP was found in the cytoplasm of the tumour cells (Figure 1a) and the distribution of LGALS3BP expression throughout the analysed samples was predominantly high, with a median of 83% (Figure 1b). Therefore, tumours whose percentage of stained

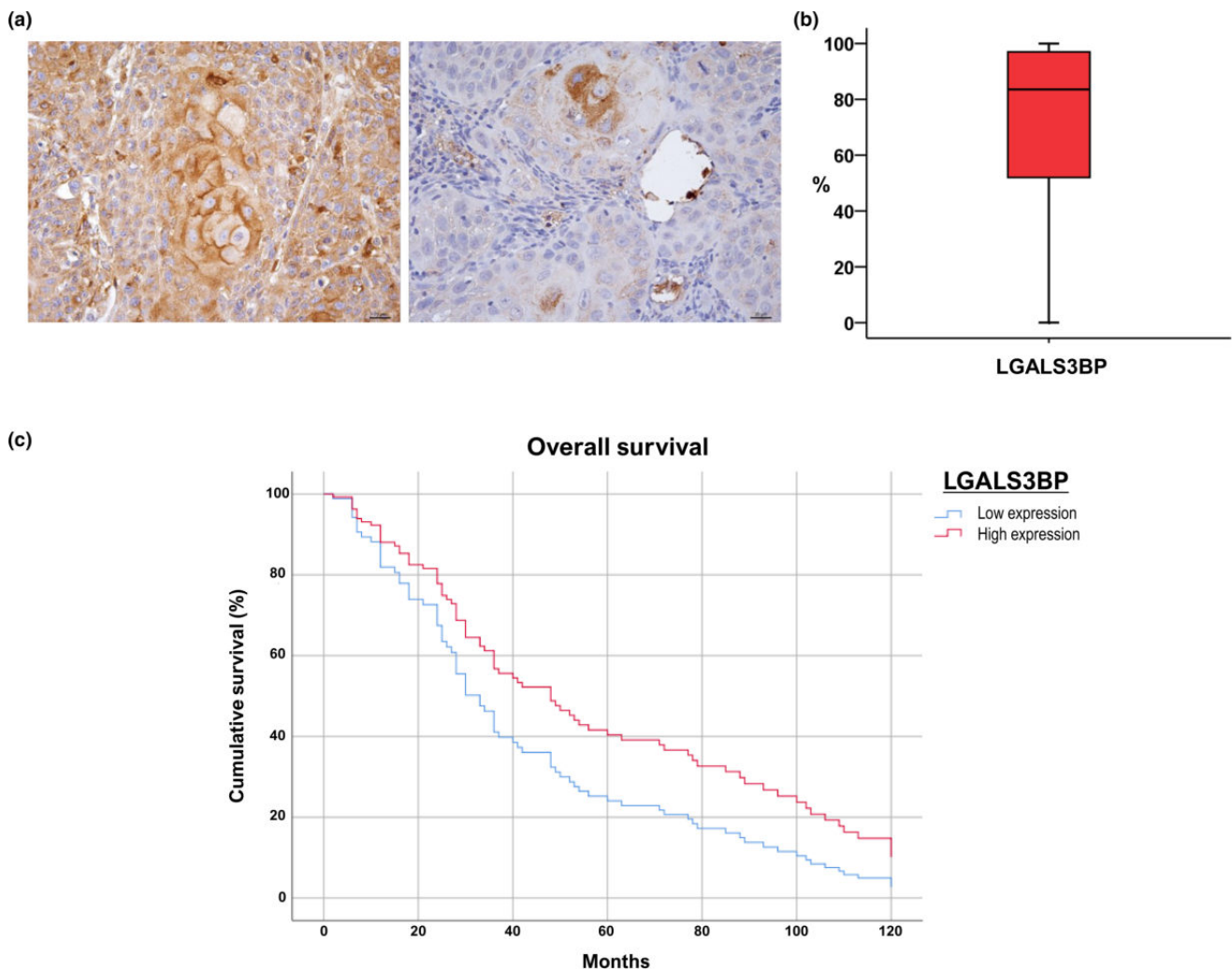


FIGURE 1 LGALS3BP expression in OSCC patient tissue samples. (a) Representative images of immunohistochemical LGALS3BP expression in tumour samples from patients ($n=98$) affected by oral squamous cell carcinoma (OSCC). Scale bar = 20 μm . (b) Box-and-whisker diagram of LGALS3BP distribution in OSCC cases ($n=98$). The upper and lower ends of the boxes represent the 75th and 25th percentiles, respectively. The median value is shown with a solid line. (c) Kaplan–Meier analysis representing overall survival (OS) of OSCC patients in relation to LGALS3BP low- or high-expressing subgroups.

TABLE 2 LGALS3BP status according to the clinical-pathological features of OSCC patients.

Variable	LGALS3BP		p-value
	Low: n (%)	High: n (%)	
Gender			
Male	41 (51.9)	38 (48.1)	0.610
Female	8 (42.1)	11 (57.9)	
Age			
Young (≤60years)	15 (46.9)	17 (53.1)	0.615
Old (>60years)	34 (52.3)	31 (47.7)	
Tumour location			
Tongue	31 (49.2)	32 (50.8)	0.794
Gingiva	1 (50.0)	1 (50.0)	
Mouth's floor	5 (62.5)	3 (37.5)	
Palate	1 (100.0)	0 (0.0)	
Cheek	11 (45.8)	13 (54.2)	
Tumour stage			
I	16 (59.3)	11 (40.7)	0.312
II	13 (59.1)	9 (40.9)	
III	8 (44.4)	10 (55.6)	
IV	11 (37.9)	18 (62.1)	
Tumour grade			
1	15 (62.5)	9 (37.5)	0.164
2	25 (53.2)	22 (46.8)	
3	9 (36.0)	16 (64.0)	
LVI			
Absent	46 (52.3)	42 (47.7)	0.317
Present	3 (33.3)	6 (66.7)	
DOI (mm)			
<5	13 (52.0)	12 (48.0)	0.835
5–10	11 (55.0)	9 (45.0)	
>10	2 (40.0)	3 (60.0)	
WPOI			
Grade 1–3	44 (57.9)	32 (42.1)	0.006*
Grade 4–5	5 (23.8)	16 (76.2)	

Abbreviations: DOI, depth of invasion; LVI, lymphovascular invasion; WPOI, worst pattern of invasion.

*Statistically significant.

cells was ≤83% were considered as low-expressing LGALS3BP, while all the others were considered high-expressing LGALS3BP. High LGALS3BP expression level was significantly associated with aggressive behaviour of OSCC in terms of the worst pattern of invasion (WPOI) ($p=0.006$) (Table 2). At Kaplan–Meier analysis, LGALS3BP expression did not affect the OS of patients with OSCC (Figure 1c). Multivariate Cox regression analysis for OS indicated as independent statistically significant prognostic factors the overall pattern of invasion (POI) and age. In particular, advanced POI was associated with a decrease in OS (Hazard Ratio 3.82, 95% Confidence Interval 1.628–8.971, p -value=0.002) as well as advanced

TABLE 3 Results from multivariate Cox regression analysis related to overall survival (OS) of patients with oral squamous cell carcinoma (OSCC).

	p-value	Hazard ratio	95.0% CI	
			Lower	Upper
LGALS3BP—low expression versus high expression	0.087	0.637	0.380	1.067
Age—old versus young	0.045*	1.020	1.000	1.039
LVI—presence versus absence	0.085	2.488	0.883	7.006
POI overall	0.021*			
POI2 vs POI1	0.740	1.127	0.555	2.291
POI3 vs POI1	0.165	1.479	0.851	2.572
POI4 vs POI1	0.002*	3.822	1.628	8.971
T overall	0.114			
T2 vs T1	0.389	0.776	0.436	1.381
T3 vs T1	0.103	1.810	0.888	3.692
T4 vs T1	0.591	1.250	0.554	2.824

Abbreviations: LVI, lymphovascular invasion; POI, pattern of invasion; T, Tumoural dimensions.

*Statistically significant.

age (Hazard Ratio 1.020, 95% Confidence Interval 1.000–1.039, p -value=0.045) (Table 3).

3.2 | In-vitro evaluation of LGALS3BP expression in OSCC cell lines

Since the heterogeneous nature of OSCC, LGALS3BP expression levels were analysed in a panel of OSCC cell lines generated from diverse sites of the oral cavity, specifically from the tongue (HSC3, HSC4, CAL27, HOC621, SAS), mouth floor (HSC2) and salivary glands (A253) (Bierbaumer et al., 2018). Intracellular as well as secreted protein levels together with mRNA expression of LGALS3BP were evaluated in OSCC cell lines and compared with hGF, a normal primary gingival fibroblast cell line. While LGALS3BP was nearly undetectable both at mRNA and protein levels in normal hGF cells (Figure 2a–d), intracellular (Figure 2a,b) and secreted (Figure 2d) LGALS3BP displayed a heterogeneous expression pattern among the different OSCC cell lines, with the highest expression level detected in HOC621 and CAL27 cell lines. Moreover, for each OSCC cell line, intracellular levels of LGALS3BP positively correlated with secreted levels measured in culture media (Figure 2b–d), suggesting that cytosolic LGALS3BP is proportionally released into the extracellular milieu.

3.3 | LGALS3BP is present and highly enriched in EVs derived from OSCC cells

We next analysed EVs-associated LGALS3BP in the same panel of OSCC cell lines. To this scope, EVs were isolated from the culture

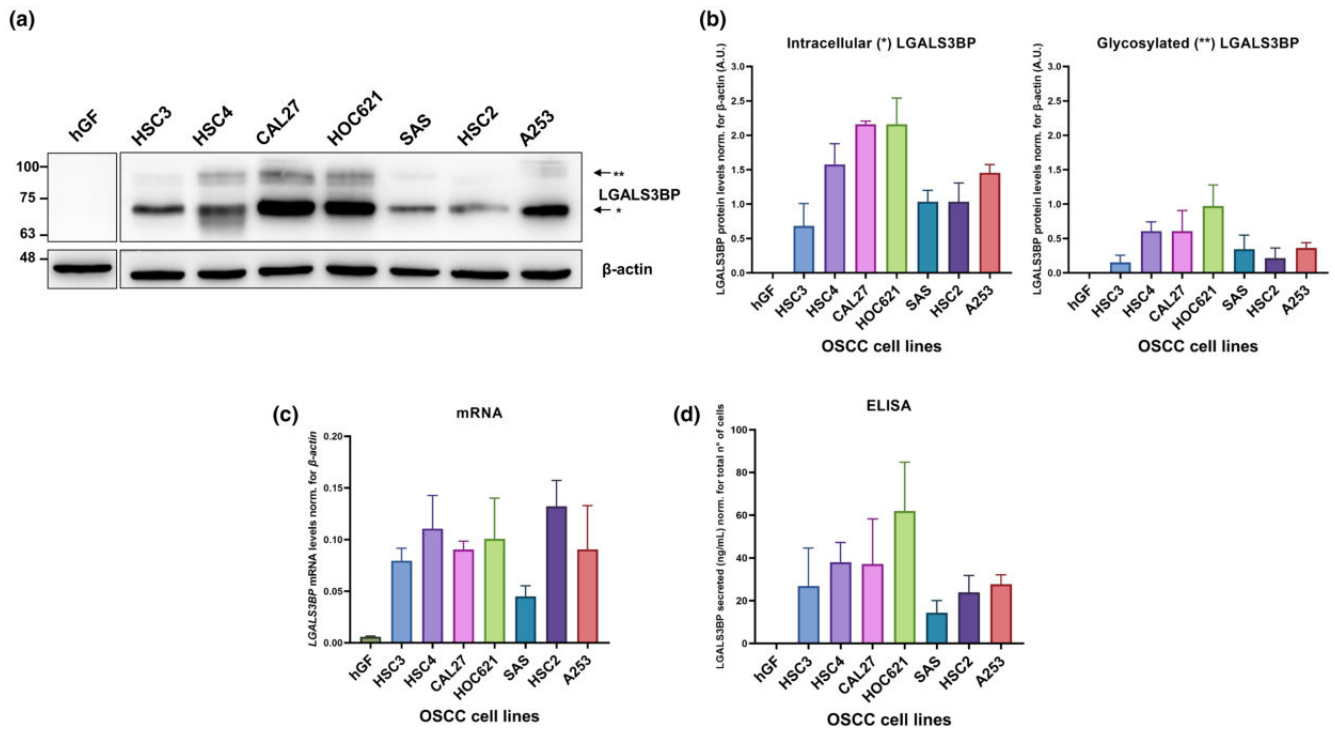


FIGURE 2 Human LGALS3BP is heterogeneously expressed and secreted in a panel of oral squamous cell carcinoma (OSCC) cell lines. (a) Western blot images showing LGALS3BP protein levels in hGF and OSCC cell lines. 20 µg of total cell lysates were loaded for each sample. β-actin was used as a loading control. WB images are representative of three independent experiments. Arrows indicate the intracellular (*, ~70kDa) and the glycosylated form (**, ~90kDa) of LGALS3BP. (b) Histograms representing protein quantification, obtained from densitometry analysis of WB images, normalized to β-actin (loading control) of intracellular (*, ~70kDa) (left) and glycosylated (**, ~90kDa) (right) LGALS3BP. Values are expressed as arbitrary units (A.U.) and are referred to means ± standard deviation (SD) (n=3). (c) Histogram representing LGALS3BP mRNA expression levels in human gingival fibroblast (hGF) and in a panel of OSCC cell lines. mRNA levels were evaluated by qRT-PCR and gene expression values were normalized relative to β-actin expression levels. Values are the means ± SD (n=3). (d) Histogram representing secreted LGALS3BP levels (ng/mL) in hGF and OSCC cell culture supernatants evaluated by ELISA assay and normalized for the total number of cells (x10⁶) harvested at the end of the experiment. Values are the means ± SD (n=3).

supernatants of OSCC cell lines and analysis of LGALS3BP levels in EVs was performed, besides their corresponding whole-cell lysates (Figure 3a,b). As a confirmation of proper EVs isolation, CD63 and CD9 tetraspanins together with β-actin levels were used as EVs markers which resulted in differently enriched in OSCC-derived EVs compared to corresponding intracellular levels (Figure 3a,b). More importantly, these data showed that 90kDa-glycosylated LGALS3BP was enriched in OSCC-derived EVs exhibiting a variable expression among the different OSCC cell lines (Figure 3a). Of note, EVs derived from HSC3, CAL27, HOC621 and HSC2 cell lines showed higher LGALS3BP content compared to HSC4-, SAS- and A253-derived EVs (Figure 3a).

Previously, it has been demonstrated that the proteins LMAN1/ERGIC-53 and MCFD2 are involved in the intracellular trafficking of LGALS3BP functioning as a transport complex crucial for LGALS3BP extracellular secretion (Chen et al., 2013; Fukamachi et al., 2018). In particular, it has been recently shown that LGALS3BP secretion levels positively correlated with levels of both MCFD2 and LMAN1 proteins in OSCC (Fukamachi et al., 2018). Therefore, the occurrence of a correlation between extracellular LGALS3BP and LMAN1/MCFD2 levels in our cell models has been explored and, with this

aim, LMAN1 and MCFD2 protein levels in the same panel of OSCC cell lines were evaluated (Figure 3c). Western blot did not show a correlation between extracellular LGALS3BP and LMAN1/MCFD2 cytosolic levels; however, a positive correlation could be assumed for HSC4 and HOC621 cell lines in which high levels of LMAN1 and MCFD2 (Figure 3c) corresponded to a higher secretion of LGALS3BP (Figure 2d).

3.4 | OSCC cells are sensitive to cytotoxic payload employed in ADC-based target therapy

Our group has recently developed an ADC specifically targeting LGALS3BP that showed potent therapeutical efficacy in different tumoural contexts, as shown in our previous works (Capone et al., 2020; Dufrusine et al., 2023; Giansanti et al., 2019). Given the high expression of LGALS3BP even in OSCC, we tested the potential applicability of the ADC therapy developed in our laboratory on OSCC cellular models. In particular, we evaluated the intrinsic sensitivity of CAL27 and HOC621, those OSCC cell lines that showed the highest LGALS3BP expression, to the payload

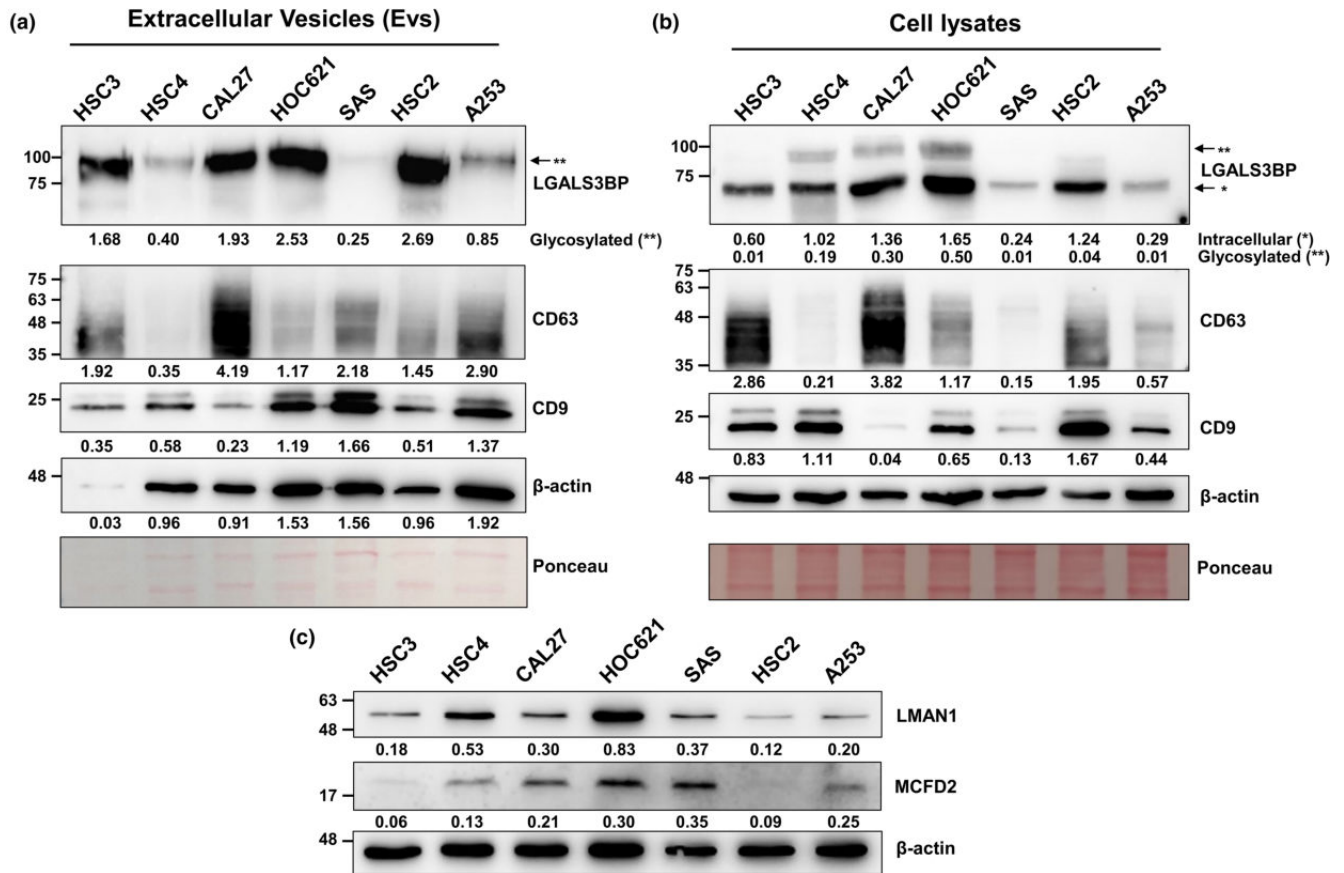


FIGURE 3 LGALS3BP is an EVs-associated protein and heterogeneously expressed in a panel of OSCC cell lines but its levels do not directly correlate with its intracellular transporters, LMAN1 and MCFD2. Western blot images showing LGALS3BP protein levels in isolated EVs (a) and corresponding whole-cell lysates (b) of OSCC cell lines. 2 μ g of EVs and 20 μ g of total cell lysates were loaded for each sample. Glycosylated (**) LGALS3BP is enriched in isolated EVs (a), while both intracellular (*) and glycosylated (**) forms of LGALS3BP are present in whole-cell lysates (b). CD63, CD9 and β -actin levels were evaluated as EV markers. Blot membranes stained with ponceau were reported as loading controls. For each protein probed, protein bands were quantified through densitometry analysis of WB images and levels were reported below each blot as raw arbitrary units (a) or normalized for β -actin levels (b). (c) Western Blot images of LMAN1 and MCFD2 protein levels in OSCC cell lines. 20 μ g of total lysates were loaded for each sample. β -actin was used as a loading control. WB images are representative of three independent experiments. Densitometry of LMAN1 and MCFD2 levels on WB images are reported below each corresponding blot as arbitrary units normalized for β -actin levels.

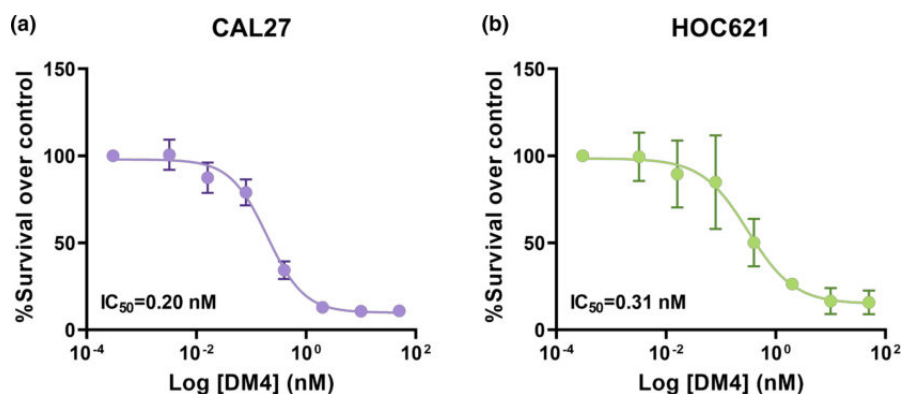


FIGURE 4 In vitro sensitivity to SH-DM4 of high-expressing LGALS3BP OSCC cell lines. (a) CAL27 and (b) HOC621 cells were treated with increasing doses of SH-DM4 for 72 h and cell-killing activity was evaluated by MTT assay. Means of percentages of survival over control are represented \pm SD of three independent experiments ($n=3$). IC₅₀ values are reported for each graph and were calculated using GraphPad Prism 9.0 software.

of our ADC corresponding to SH-DM4 drug, which exerts its cytotoxic activity since it is a potent inhibitor of tubulin polymerization. As reported in Figure 4, OSCC cells showed a strong sensitivity with IC₅₀ values of 0.2 and 0.3 nM, respectively, as assessed by MTT assay.

4 | DISCUSSION

The development of novel therapeutic strategies for OSCC treatment is an urgent need, and given the LGALS3BP potential as a druggable target, in this work, we have evaluated tissue LGALS3BP



expression levels in a cohort of OSCC patients as well as its intracellular and EVs-associated expression patterns in a panel of available cell lines. Two general observations derive from these data: LGALS3BP is highly expressed in OSCC promoting a more aggressive phenotype, and EVs derived from OSCC cell lines are enriched with LGALS3BP. The first consideration derives from the evidence that more than 95% of the analyzed OSCC patients were positive for LGALS3BP, though with variable expression. This is in line with other observations from the literature in which LGALS3BP levels are high in a wide variety of cancer tissues; instead, its expression is minimal or undetectable in normal tissues (Capone et al., 2021; Fukamachi et al., 2018; Giansanti et al., 2019; Ulmer et al., 2006). We were able to dichotomize OSCC patients into low- and high-expressing LGALS3BP groups. Multivariate Cox regression analysis showed that LGALS3BP expression did not influence the OS; however, we observed a trend for which high expression levels of LGALS3BP correlated with better prognosis. Instead, in a similar previous study, Zhang et al. found that IHC expression was an independent adverse factor for OS and relapse-free survival in a cohort of 92 OSCC patients (Zhang et al., 2019). While more studies support a negative impact of LGALS3BP overexpression on patients' outcomes and tumour characteristics (He et al., 2019; Iacobelli et al., 1994; Marchetti et al., 2002; Sun et al., 2013; Tinari et al., 2009; Zeimet et al., 1996; Zhang et al., 2019), evidence for which LGALS3BP is associated with favourable clinical outcome was reported for colorectal carcinoma (Piccolo et al., 2015), pleural mesothelioma (Strizzi et al., 2002) and Ewing's sarcoma (Zambelli et al., 2010), suggesting that, likely due to the versatile multifunctionality of this protein, LGALS3BP might have a controversial prognosis-related role depending on the cancer type and spatial allocation, in terms of cytoplasmatic, interstitial secretion and serum delivering of this protein.

The second observation we brought in this work is the evidence that LGALS3BP is highly and differently expressed in OSCC cells and more importantly enriched in cancer-derived EVs, strengthening the notion of its specific functional role as a vesicular protein. However, our results highlight that LGALS3BP expression levels significantly changed among the cell lines. This phenomenon was already observed in other types of cancer, such as neuroblastoma or glioblastoma as recently shown by our groups (Capone et al., 2020; Dufrusine et al., 2023). Yet, heterogeneous pattern of expression of LGALS3BP and mechanisms implicated in its expression and secretion is not fully understood. To date, some works have proposed that LGALS3BP secretion might involve interaction with LMAN1, an Endoplasmic Reticulum (ER)-Golgi transporter molecule that recognizes high-mannose type N-glycans; this means that N-glycosylation of LGALS3BP appears to be essential for its secretion (Chen et al., 2013). In addition to this transmembrane protein, another LGALS3BP-interactor, named MCFD2, allows in concert with LMAN1 the transport from the ER to the Golgi where post-translational changes occur. Of note, Fukamachi et al. reported co-upregulation of LGALS3BP and MCFD2 in OSCC, and patients harbouring this dysregulation were more likely

to develop lymph nodes metastasis (Fukamachi et al., 2018). In our OSCC models, we did not observe a close correlation between intracellular transporters LMAN1/MCFD2 and LGALS3BP levels, nor with EVs-associated LGALS3BP content (Figure 3), indicating that LGALS3BP of EVs compartment may not directly depend on the LMAN1-MCFD2 intracellular transport complex along the secretory pathway.

Given its overexpression in tumour tissue and its abundance and accumulation in extracellular stroma also as EVs-associated protein, LGALS3BP lends itself to being a promising druggable target, especially for antibody-based therapy with non-internalizing ADCs (Capone et al., 2020, 2021; Choi et al., 2022; Dufrusine et al., 2023; Giansanti et al., 2019; Hee Lee et al., 2013). In this context, the most attractive feature of targeting extracellular LGALS3BP with 1959-sss/DM4 in the tumour microenvironment is that this strategy may induce a potent antitumour activity through the direct killing of both cancer and stroma cells. Indeed, this bystander effect is made possible by the lipophilic nature of the cytotoxic payload, which enhances the passive uptake of the drug by cancer cells as well as by TME-associated cells. However, detailed molecular mechanisms of action beyond the effectiveness of 1959-sss/DM4 ADC are still under investigation. Thus, in this work, the emerged evidence from our results that LGALS3BP is overexpressed in almost all OSCC patients and cell line models lay the foundations for testing our ADC targeting this protein as a novel therapeutic strategy for OSCC. To complete the favourable picture, preliminary assays showed OSCC cell lines to be highly susceptible to the payload loaded onto the anti-LGALS3BP ADC (1959-sss/DM4) in the range of nanomolar scale (Figure 4) (Capone et al., 2020; Dufrusine et al., 2023; Giansanti et al., 2019) suggesting that generation of OSCC pre-clinical models would be the needed next step to further evaluate the therapeutic potential of DM4-based anti-LGALS3BP ADC.

5 | CONCLUSIONS

LGALS3BP prognostic value and functional mechanism in OSCC are still unclear. Further investigations will be crucial to better understand the association between LGALS3BP levels and cancer progression even in OSCC to pave the way for the development and translational application of innovative and more effective therapeutic approaches. In sum, our data indicate that LGALS3BP is highly expressed in OSCC and represents a potential target for ADC-based therapy. Therapeutic studies are necessary to confirm LGALS3BP as a promising target for cancer immunotherapy in OSCC.

AUTHOR CONTRIBUTIONS

Ilaria Cela: Investigation; formal analysis; data curation; methodology; writing – original draft. **Vito Carlo Alberto Caponio:** Writing – original draft; formal analysis; data curation. **Emily Capone:** Investigation; writing – review and editing; data curation. **Morena Pinti:** Investigation. **Marco Mascitti:** Writing – review and editing; formal analysis;

resources. **Lucrezia Togni**: Data curation; methodology. **Lorenzo Lo Muzio**: Data curation; writing – review and editing. **Corrado Rubini**: Data curation; writing – review and editing; resources. **Vincenzo De Laurenzi**: Writing – review and editing; funding acquisition. **Rossano Lattanzio**: Data curation; formal analysis; investigation; methodology. **Vittoria Perrotti**: Conceptualization; writing – original draft; supervision; writing – review and editing. **Gianluca Sala**: Conceptualization; writing – original draft; supervision; writing – review and editing; funding acquisition; project administration.

ACKNOWLEDGMENTS

We thank all medical doctors, nurses and patients who were involved in the collection of the samples. Francesco Del Pizzo is kindly acknowledged for helping with the immunohistochemistry assays.

FUNDING INFORMATION

This study was financially supported by Fondazione-AIRC: GS (IG 2021 id 25696), VdL (IG 2018 id 20043). The research leading to these results has received funding from the European Union–NextGenerationEU through the Italian Ministry of University and Research under PNRR–M4C2-I1.3 Project PE_00000019 ‘HEAL ITALIA HEALTH EXTENDED ALLIANCE FOR INNOVATIVE THERAPIES, ADVANCED LAB-RESEARCH, AND INTEGRATED APPROACHES OF PRECISION MEDICINE’ to Vito Carlo Alberto Caponio and Lorenzo Lo Muzio CUP D73C22001230006. The views and opinions expressed are those of the authors only and do not necessarily reflect those of the European Union or the European Commission.

CONFLICT OF INTEREST STATEMENT

None of the authors has a conflict of interest to declare.

DATA AVAILABILITY STATEMENT

The data that support the findings of this study are available from the corresponding author upon reasonable request.

ORCID

Ilaria Cela  <https://orcid.org/0000-0003-3122-2688>

Vito Carlo Alberto Caponio  <https://orcid.org/0000-0001-5080-5921>

Lorenzo Lo Muzio  <https://orcid.org/0000-0003-4633-4893>

Rossano Lattanzio  <https://orcid.org/0000-0001-9803-4476>

Gianluca Sala  <https://orcid.org/0000-0002-4494-915X>

REFERENCES

- Bierbaumer, L., Schwarze, U. Y., Gruber, R., & Neuhaus, W. (2018). Cell culture models of Oral mucosal barriers: A review with a focus on applications, culture conditions and barrier properties. *Tissue Barriers*, 6, 1479568. <https://doi.org/10.1080/21688370.2018.1479568>
- Capone, E., Iacobelli, S., & Sala, G. (2021). Role of galectin 3 binding protein in cancer progression: A potential novel therapeutic target. *Journal of Translational Medicine*, 19, 405. <https://doi.org/10.1186/S12967-021-03085-W>
- Capone, E., Lamolinara, A., Pastorino, F., Gentile, R., Ponziani, S., Di Vittorio, G., D'agostino, D., Bibbò, S., Rossi, C., Piccolo, E., Iacobelli, V., Lattanzio, R., Panella, V., Sallèse, M., De Laurenzi, V., Giansanti, F., Sala, A., Iezzi, M., Ponzoni, M., Ippoliti, R., ... Sala, G. (2020). Targeting vesicular LGALS3BP by an antibody-drug conjugate as novel therapeutic strategy for neuroblastoma. *Cancers (Basel)*, 12, 1–18. <https://doi.org/10.3390/CANCERS12102989>
- Castillo, J., Bernard, V., San Lucas, F. A., Allenson, K., Capello, M., Kim, D. U., Gascoyne, P., Mulu, F. C., Stephens, B. M., Huang, J., Wang, H., Momin, A. A., Jacamo, R. O., Katz, M., Wolff, R., Javle, M., Varadhachary, G., Wistuba, I. I., Hanash, S., ... Alvarez, H. (2018). Surfaceome profiling enables isolation of cancer-specific exosomal cargo in liquid biopsies from pancreatic cancer patients. *Annals of Oncology*, 29, 223–229. <https://doi.org/10.1093/ANNONC/MDX542>
- Chen, Y., Hojo, S., Matsumoto, N., & Yamamoto, K. (2013). Regulation of mac-2BP secretion is mediated by its N-glycan binding to ERGIC-53. *Glycobiology*, 23, 904–916. <https://doi.org/10.1093/GLYCOB/CWT027>
- Choi, Y. S., Kim, M. J., Choi, E. A., Kim, S., Lee, E. J., Park, M. J., Kim, M. J., Kim, Y. W., Ahn, H. S., Jung, J. Y., Jang, G., Kim, Y., Kim, H., Kim, K., Kim, J. Y., Hong, S. M., Kim, S. C., & Chang, S. (2022). Antibody-mediated blockade for galectin-3 binding protein in tumor secretome abrogates PDAC metastasis. *Proceedings of the National Academy of Sciences of the United States of America*, 119, e2119048119. <https://doi.org/10.1073/PNAS.2119048119/-DCSUPPLEMENTAL>
- Dufrusine, B., Capone, E., Ponziani, S., Lattanzio, R., Lanuti, P., Giansanti, F., de Laurenzi, V., Iacobelli, S., Ippoliti, R., Mangiola, A., Trevisi, G., & Sala, G. (2023). Extracellular LGALS3BP: A potential disease marker and actionable target for antibody-drug conjugate therapy in glioblastoma. *Molecular Oncology*, 17, 1460–1473. <https://doi.org/10.1002/1878-0261.13453>
- Endo, H., Muramatsu, T., Furuta, M., Uzawa, N., Pimkhaokham, A., Amagasa, T., Inazawa, J., & Kozaki, K. (2013). Ichi potential of tumor-suppressive MiR-596 targeting LGALS3BP as a therapeutic agent in oral cancer. *Carcinogenesis*, 34, 560–569. <https://doi.org/10.1093/CARCIN/BGS376>
- Escrevente, C., Grammel, N., Kandzia, S., Zeiser, J., Tranfield, E. M., Conradt, H. S., & Costa, J. (2013). Sialoglycoproteins and N-glycans from secreted exosomes of ovarian carcinoma cells. *PLoS One*, 8, e78631. <https://doi.org/10.1371/JOURNAL.PONE.0078631>
- Fornarini, B., D'Ambrosio, C., Natoli, C., Tinari, N., Silingardi, V., & Iacobelli, S. (2000). Adhesion to 90K (Mac-2 BP) as a mechanism for lymphoma drug resistance in vivo. *Blood*, 96(9), 3282–3285.
- Fukamachi, M., Kasamatsu, A., Endo-Sakamoto, Y., Fushimi, K., Kasama, H., Iyoda, M., Minakawa, Y., Shiiba, M., Tanzawa, H., & Uzawa, K. (2018). Multiple coagulation factor deficiency protein 2 as a crucial component in metastasis of human oral cancer. *Experimental Cell Research*, 368, 119–125. <https://doi.org/10.1016/J.YEXCR.2018.04.021>
- Giansanti, F., Capone, E., Ponziani, S., Piccolo, E., Gentile, R., Lamolinara, A., di Campli, A., Sallèse, M., Iacobelli, V., Cimini, A., de Laurenzi, V., Lattanzio, R., Piantelli, M., Ippoliti, R., Sala, G., & Iacobelli, S. (2019). Secreted gal-3BP is a novel promising target for non-internalizing antibody-drug conjugates. *Journal of Controlled Release*, 294, 176–184. <https://doi.org/10.1016/J.JCONREL.2018.12.018>
- He, X., Zhang, S., Chen, J., & Li, D. (2019). Increased LGALS3 expression independently predicts shorter overall survival in patients with the proneural subtype of glioblastoma. *Cancer Medicine*, 8, 2031–2040. <https://doi.org/10.1002/CAM4.2075>



- Hee Lee, J., Park, M. S., Hwang, J. E., Cho, S. H., Bae, W. K., Shim, H. J., Kim, D. E., & Chung, I. J. (2013). Dendritic cell-based immunotherapy for colon cancer using an HLA-A*0201-restricted cytotoxic T-lymphocyte epitope from tumor-associated antigen 90K. *Cellular & Molecular Immunology*, 10, 275–282. <https://doi.org/10.1038/CMI.2012.74>
- Iacobelli, S., Sisoni, P., Giai, M., D'Egidio, M., Tinari, N., Amatetti, C., Di Stefano, P., & Natoli, C. (1994). Prognostic value of a novel circulating serum 90K antigen in breast cancer. *British Journal of Cancer*, 69, 172–176. <https://doi.org/10.1038/BJC.1994.29>
- Keinänen, O., Sarrett, S. M., Delaney, S., Rodriguez, C., Days, E. J., Capone, E., Sauniere, F., Ippoliti, R., Sala, G., Iacobelli, S., & Zeglis, B. M. (2023). Visualizing galectin-3 binding protein expression with immunoPET. *Molecular Pharmaceutics*, 20, 3241–3248. <https://doi.org/10.1021/ACS.MOLPHARMACEUT.3C00241>
- Marchetti, A., Tinari, N., Buttitta, F., Chella, A., Angeletti, C. A., Rocco, S., Mucilli, F., Ullrich, A., & Iacobelli, S. (2002). Expression of 90K (mac-2 BP) correlates with distant metastasis and predicts survival in stage I non-small cell lung cancer patients cancer cell signaling view project tyrosine kinase receptors view project. *Cancer Research*, 62, 2535–2539.
- Mascitti, M., Togni, L., Caponio, V. C. A., Zhurakivska, K., Bizzoca, M. E., Contaldo, M., Serpico, R., Lo Muzio, L., & Santarelli, A. (2022). Lymphovascular invasion as a prognostic tool for oral squamous cell carcinoma: A comprehensive review. *International Journal of Oral and Maxillofacial Surgery*, 51, 1–9. <https://doi.org/10.1016/j.ijom.2021.03.007>
- Mascitti, M., Zhurakivska, K., Togni, L., Caponio, V. C. A., Almangush, A., Balercia, P., Balercia, A., Rubini, C., Lo Muzio, L., Santarelli, A., & Troiano, G. (2020). Addition of the tumour-stroma ratio to the 8th edition American Joint Committee on cancer staging system improves survival prediction for patients with Oral tongue squamous cell carcinoma. *Histopathology*, 77, 810–822. <https://doi.org/10.1111/HIS.14202>
- Nakata, R., Shimada, H., Fernandez, G. E., Fanter, R., Fabbri, M., Malvar, J., Zimmermann, P., & DeClerck, Y. A. (2017). Contribution of neuroblastoma-derived exosomes to the production of pro-tumorigenic signals by bone marrow mesenchymal stromal cells. *Journal of Extracellular Vesicles*, 6, 1332941. <https://doi.org/10.1080/20013078.2017.1332941>
- Ozaki, Y., Kontani, K., Teramoto, K., Fujita, T., Tezuka, N., Sawai, S., Maeda, T., Watanabe, H., Fujino, S., Asai, T., & Ohkubo, I. (2004). Involvement of 90K/mac-2 binding protein in cancer metastases by increased cellular adhesiveness in lung cancer. *Oncology Reports*, 12, 1071–1077. <https://doi.org/10.3892/or.12.5.1071>
- Park, Y. P., Choi, S. C., Kim, J. H., Song, E. Y., Kim, J. W., Yoon, D. Y., Yeom, Y. I., Lim, J. S., Kim, J. W., Paik, S. G., & Lee, H. G. (2007). Up-regulation of mac-2 binding protein by HTERT in gastric cancer. *International Journal of Cancer*, 120, 813–820. <https://doi.org/10.1002/IJC.22369>
- Perrotti, V., Caponio, V. C. A., Mascitti, M., Lo Muzio, L., Piattelli, A., Rubini, C., Capone, E., & Sala, G. (2021). Therapeutic potential of antibody-drug conjugate-based therapy in head and neck cancer: A systematic review. *Cancers (Basel)*, 13, 3126. <https://doi.org/10.3390/CANCERS13133126>
- Piccolo, E., Tinari, N., D'Addario, D., Rossi, C., Iacobelli, V., la Sorda, R., Lattanzio, R., D'Egidio, M., di Risio, A., Piantelli, M., Natali, P. G., & Iacobelli, S. (2015). Prognostic relevance of LGALS3BP in human colorectal carcinoma. *Journal of Translational Medicine*, 13, 248. <https://doi.org/10.1186/S12967-015-0606-X>
- Singh, P., Verma, J. K., & Singh, J. K. (2020). Validation of salivary markers, IL-1 β , IL-8 and Lgals3bp for detection of oral squamous cell carcinoma in an Indian population. *Scientific Reports*, 10, 7365. <https://doi.org/10.1038/S41598-020-64494-3>
- Song, Y., Wang, M., Tong, H., Tan, Y., Hu, X., Wang, K., & Wan, X. (2021). Plasma exosomes from endometrial cancer patients contain LGALS3BP to promote endometrial cancer progression. *Oncogene*, 40, 633–646. <https://doi.org/10.1038/S41388-020-01555-X>
- Strizzi, L., Muraro, R., Vianale, G., Natoli, C., Talone, L., Catalano, A., Mutti, L., Tassi, G., & Procopio, A. (2002). Expression of glycoprotein 90K in human malignant pleural mesothelioma: Correlation with patient survival. *The Journal of Pathology*, 197, 218–223. <https://doi.org/10.1002/PATH.1125>
- Sun, L., Chen, L., Sun, L., Pan, J., Yu, L., Han, L. L., Yang, Z., Luo, Y., & Ran, Y. (2013). Functional screen for secreted proteins by monoclonal antibody library and identification of mac-2 binding protein (mac-2BP) as a potential therapeutic target and biomarker for lung cancer. *Molecular & Cellular Proteomics*, 12, 395–406. <https://doi.org/10.1074/MCP.M112.020784>
- Tinari, N., Lattanzio, R., Querzoli, P., Natoli, C., Grassadonia, A., Alberti, S., Hubalek, M., Reimer, D., Nenci, I., Bruzzi, P., Piantelli, M., Iacobelli, S., & on behalf of the Consorzio Interuniversitario Nazionale per la Bio-Oncologia (CINBO). (2009). High expression of 90K (mac-2 BP) is associated with poor survival in node-negative breast cancer patients not receiving adjuvant systemic therapies. *International Journal of Cancer*, 124, 333–338. <https://doi.org/10.1002/IJC.23970>
- Togni, L., Caponio, V. C. A., Zerman, N., Troiano, G., Zhurakivska, K., Lo Muzio, L., Balercia, A., Mascitti, M., & Santarelli, A. (2022). The emerging impact of tumor budding in oral squamous cell carcinoma: Main issues and clinical relevance of a new prognostic marker. *Cancers (Basel)*, 14, 3571. <https://doi.org/10.3390/CANCERS14153571>
- Traini, S., Piccolo, E., Tinari, N., Rossi, C., la Sorda, R., Spinella, F., Bagnato, A., Lattanzio, R., D'Egidio, M., di Risio, A., Tomao, F., Grassadonia, A., Piantelli, M., Natoli, C., & Iacobelli, S. (2014). Inhibition of tumor growth and angiogenesis by SP-2, an anti-lectin, galactoside-binding soluble 3 binding protein (LGALS3BP) antibody. *Molecular Cancer Therapeutics*, 13, 916–925. <https://doi.org/10.1158/1535-7163.MCT-12-1117>
- Ulmer, T. A., Keeler, V., Loh, L., Chibbar, R., Torlakovic, E., André, S., Gabius, H. J., & Laferté, S. (2006). Tumor-associated antigen 90K/mac-2-binding protein: Possible role in colon cancer. *Journal of Cellular Biochemistry*, 98, 1351–1366. <https://doi.org/10.1002/JCB.20784>
- Weng, L. P., Wu, C. C., Hsu, B. L., Chi, L. M., Liang, Y., Tseng, C. P., Hsieh, L. L., & Yu, J. S. (2008). Secretome-based identification of mac-2 binding protein as a potential oral cancer marker involved in cell growth and motility. *Journal of Proteome Research*, 7, 3765–3775. <https://doi.org/10.1021/PR800042N>
- Yu, J. S., Chen, Y. T., Chiang, W. F., Hsiao, Y. C., Chu, L. J., See, L. C., Wu, C. S., Tu, H. T., Chen, H. W., Chen, C. C., Liao, W. C., Chang, Y. T., Wu, C. C., Lin, C. Y., Liu, S. Y., Chiou, S. T., Chia, S. L., Chang, K. P., Chien, C. Y., ... Hartwell, L. H. (2016). Saliva protein biomarkers to detect oral squamous cell carcinoma in a high-risk population in Taiwan. *Proceedings of the National Academy of Sciences of the United States of America*, 113, 11549–11554. <https://doi.org/10.1073/PNAS.1612368113>
- Zambelli, D., Zuntini, M., Nardi, F., Manara, M. C., Serra, M., Landuzzi, L., Lollini, P. L., Ferrari, S., Alberghini, M., Lombart-Bosch, A., Piccolo, E., Iacobelli, S., Picci, P., & Scotlandi, K. (2010). Biological indicators of prognosis in Ewing's sarcoma: An emerging role for lectin galactoside-binding soluble 3 binding protein (LGALS3BP). *International Journal of Cancer*, 126, 41–52. <https://doi.org/10.1002/IJC.24670>
- Zeimet, A. G., Natoli, C., Herold, M., Fuchs, D., Windbichler, G., Daxenbichler, G., Iacobelli, S., Dapunt, O., & Marth, C. (1996). Circulating Immunostimulatory protein 90K and soluble interleukin-2-receptor in human ovarian cancer. *International Journal of Cancer*, 68, 34–38. [https://doi.org/10.1002/\(sici\)1097-0215\(19960927\)68:1<34::aid-ijc7>3.0.co;2-y](https://doi.org/10.1002/(sici)1097-0215(19960927)68:1<34::aid-ijc7>3.0.co;2-y)

- Zhang, X., Ding, H., Lu, Z., Ding, L., Song, Y., Jing, Y., Hu, Q., Dong, Y., & Ni, Y. (2019). Increased LGALS3BP promotes proliferation and migration of oral squamous cell carcinoma via PI3K/AKT pathway. *Cellular Signalling*, 63, 109359. <https://doi.org/10.1016/J.CELLSIG.2019.109359>
- Zhu, G., Yang, F., Wei, H., Meng, W., Gan, J., Wang, L., He, C., Lu, S., Cao, B., Luo, H., Han, B., & Li, L. (2023). 90 K increased delivery efficiency of extracellular vesicles through mediating internalization. *Journal of Controlled Release*, 353, 930–942. <https://doi.org/10.1016/J.JCONREL.2022.12.034>

How to cite this article: Cela, I., Caponio, V. C. A., Capone, E., Pinti, M., Mascitti, M., Togni, L., Lo Muzio, L., Rubini, C., De Laurenzi, V., Lattanzio, R., Perrotti, V., & Sala, G. (2024). LGALS3BP is a potential target of antibody-drug conjugates in oral squamous cell carcinoma. *Oral Diseases*, 30, 2039–2050. <https://doi.org/10.1111/odi.14719>